

Synthesis and Characterization of Superabsorbent Hydrogel from Activated Hydrochar-Sucrose Crosslinked with Maleic Acid

Stanley M. Mukulu¹, Harun M. Mbuvi¹, Titus M. Kasimu², Francis Maingi³

¹Department of Chemistry, Kenyatta University, Nairobi, Kenya

²Department of Physical Sciences, Machakos University, Machakos, Kenya

³Department of Science Technology and Engineering, Kibabii University, Bungoma, Kenya

Email: mukoramaingi@gmail.com

How to cite this paper: Mukulu, S.M., Mbuvi, H.M., Kasimu, T.M. and Maingi, F. (2026) Synthesis and Characterization of Superabsorbent Hydrogel from Activated Hydrochar-Sucrose Crosslinked with Maleic Acid. *Open Journal of Applied Sciences*, 16, 423-436.

<https://doi.org/10.4236/ojapps.2026.162026>

Received: December 7, 2025

Accepted: January 27, 2026

Published: January 30, 2026

Copyright © 2026 by author(s) and Scientific Research Publishing Inc. This work is licensed under the Creative Commons Attribution International License (CC BY 4.0).

<http://creativecommons.org/licenses/by/4.0/>



Open Access

Abstract

Superabsorbent hydrogels are hydrophilic materials forming three-dimensional polymer networks capable of absorbing large amounts of water. They are utilized in various fields, though most current types are non-biodegradable and costly to produce. This research explored a more sustainable approach by synthesizing superabsorbent hydrogels from activated hydrochar derived from sugarcane bagasse, using acidified potassium manganate for activation and sucrose for polymerization. Maleic acid was employed to create crosslinked structures, optimizing swelling capacity through varying conditions. Characterization through FT-IR confirmed successful crosslinkage. XRD analysis showed the amorphous nature of hydrochar and AH as compared to the increased crystallinity exhibited by AHSU polymer units and SAH superabsorbent hydrogel. SEM analysis revealed that the superabsorbent hydrogel had compact permeable surface network structures. The optimal synthesis ratio was found to yield a swelling capacity of 778% within 12 hours, highlighting the potential of these biocompatible hydrogels for agricultural applications in semi-arid and arid regions.

Keywords

Activated Hydrochar, Cross-Linker, Sucrose, Superabsorbent Hydrogel

1. Introduction

Superabsorbent hydrogels are three-dimensional polymer network structures

with exceptional water or aqueous solution absorption and retention properties [1]. The polymer network contains polar hydrophilic groups, which include $-OH$, $-COOH$, $-COO-Na^+$, $-CONH_2$, and $-SO_3H/-SO_3^-M^+$ [2], enabling them to absorb and retain water in their structure without dissolving. Due to increased population, the demand for hydrogels in agricultural application has enormously increased. However, the hydrogels currently available in the market are environmentally unfriendly since they have poor biodegradability [3]. Consequently, many researchers are working on developing superabsorbent hydrogels from low-cost, biocompatible, and biodegradable biomass [4]. Biodegradable hydrogels can be synthesized from carbohydrate-based polymers that are biocompatible, non-toxic, renewable, cheaper, and easy to obtain [5]. Biomass materials such as sugarcane bagasse is a waste product that is non-toxic, and biodegradable, with high cellulose content. Hydrochar is produced from biomass via dehydration process using concentrated sulphuric acid (chemical method). Due to high levels of cellulose in sugarcane bagasse, it can be used to prepare activated hydrochar monomers for synthesizing superabsorbent hydrogels [6]. This study therefore aimed at synthesizing and characterizing superabsorbent hydrogel from hydrochar using sugarcane bagasse as a resource.

2. Materials and Methods

2.1. Chemical and Reagents

The chemicals and reagents used in this study of analytical grade purchased from Amaris chemical solutions. They were sucrose, maleic acid, sodium hydroxide, potassium permanganate (VII), and concentrated sulphuric acid.

2.2. Preparation of the Hydrochar

The procedure used to prepare hydrochar was adopted from [6]. Small pieces of sugarcane bagasse were cleaned, dried. They were then placed in 1000 mL glass beaker. 100 mL of 18 M concentrated sulphuric acid was then added and allowed to stand for 30 minutes to allow complete dehydration. The char obtained was then washed with distilled water to remove excess acid and dried in an oven at $80^\circ C$ to a constant mass.

2.3. Preparation of Activated Hydrochar Sucrose Polymer Units (AHSU)

20 g of grinded fine hydrochar was put in a 1000 mL beaker. 600 mL of 2 M acidified potassium permanganate (VII) was then added and the mixture kept in a safe place for 16 hours to allow oxidation reaction to occur. The mixture was then filtered, and the residue washed with excess distilled water to remove the excess potassium permanganate (VII). The activated hydrochar (AH) obtained was then dried in an oven at $80^\circ C$. Dry activated hydrochar (AH) obtained was ground to fine powder. 20 g was accurately weighed using a CZ-200 electric weighing balance and then placed in a 250 mL round-bottomed flask. 30 mL of distilled water

was added and the mixture refluxed while stirring for 10 minutes. 10 mL of 3.5 M sucrose was then added, followed by 2 M sodium hydroxide (initiator) Refluxing of the mixture was done for 3 hours. The mixture was then allowed to cool for polymerization to occur [7]. The polymer formed between activated hydrochar and sucrose was coded as AHSU.

2.4. Crosslinking AHSU Polymer Units with Maleic Acid

The polymer units (AHSU) obtained from section 2.3 was heated to boiling. The boiling mixture was then added 10 mL of 3.4 M maleic acid (MA) and the mixture refluxed for 2 hours. The refluxed mixture was placed in an oven at 80°C to dry to a constant mass. The hot dried mixture was then placed in a desiccator to cool. The obtained crosslinked superabsorbent hydrogel was coded as SAH. **Figure 1** below shows the scheme for the synthesis of polymer units AHSU and crosslinked superabsorbent hydrogel SAH.

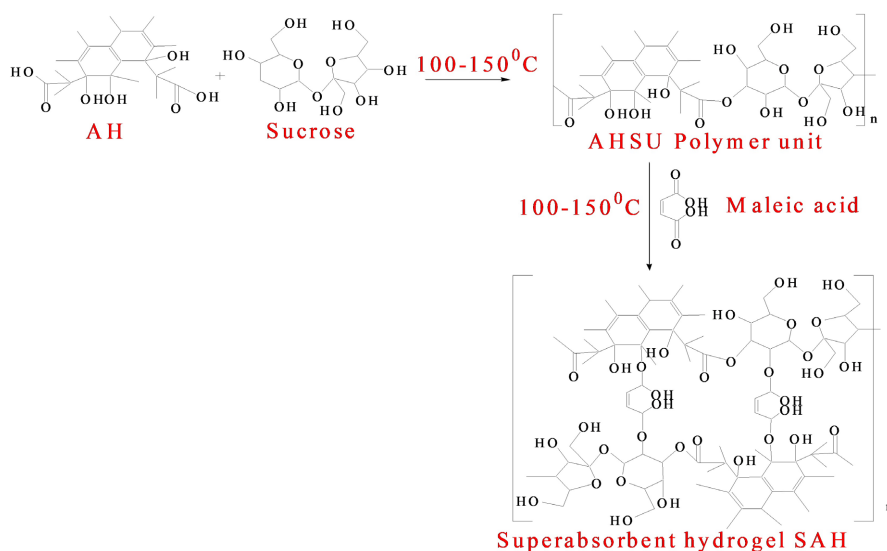


Figure 1. Scheme for the preparation of AHSU and SAH.

2.5. Evaluation of the Swelling Capacity of SAH

2.0 g of accurately weighed dry hydrogel samples were placed in permeable polyester bags, and the total mass was recorded as (M). The samples were then immersed in distilled water, and the absorption process allowed to take place for 24 hours. The bags were then removed from the water, and the adhering water on the surface of the polyester bags dried using a tissue paper. The samples were then weighed, and the mass obtained recorded as (Z). The percentage absorption capacity of the hydrogel samples was determined using Equation 1 as per Khodami *et al.* [8].

$$\% \text{ swelling capacity} = \frac{Z - M}{M} \times \% \quad (1)$$

where Z is the weight of the swollen hydrogel samples, M is the weight of the dry hydrogel samples.

2.6. Optimization of Synthesis Parameters

2.6.1. Effect of the Maleic Acid Dosages on the Swelling Capacity of SAH Hydrogel

The effect of maleic acid was evaluated by synthesising samples of the SAH with varied amounts of maleic acid ranging from 1, 2, 3, 4 and 5 g. The quantities of AH, SU and NaOH were maintained at 10 g, 5 g and 0.8 g respectively. 2 g of each prepared hydrogel samples was accurately weighed and immersed in distilled water for 24 hours and then removed to determine the swelling capacity using Equation 1.

2.6.2. Effect of the Amount of Sucrose on the Swelling Capacity of SAH Hydrogel

The effect of sucrose dosage was investigated by preparing superabsorbent hydrogel samples by varying the amount of sucrose as 2, 4, 6, 8, and 10 g, while maintaining AH, MA, and NaOH at constant masses of 10 g, 3 g, and 0.8 g, respectively. 2 g of each synthesised SAH hydrogel sample was accurately weighed and immersed in distilled water for 24 hours. Evaluation of swelling capacity was done using Equation 1.

2.6.3. Effect of Contact Time on the Swelling Capacity of SAH Hydrogel

The SAH samples synthesised at optimum conditions of sucrose and maleic doses. 2 g of the synthesized samples and put in were accurately weighed and put into permeable polyester bags and then immersed in distilled water. The bags were then removed periodically at the lapse of each designated time (0.5, 1, 2, 4, 6, 8, 12, and 24 hours). Swelling capacity of each sample was then determined using Equation 1.

2.7. Characterization of the Hydrogels

2.7.1. Functional Groups Analysis Using Fourier Transform Infrared (FT-IR)

FT-IR analysis was done to determine the functional groups of the hydrochar, AH, AHSU and SAH using FT-IR spectroscopy (Shimadzu IR Tracer-100) according to the procedure by Kulkarni *et al.* [9]. Upon synthesizing the samples, they were dried to a constant mass in an oven followed by grinding to obtain fine powder. The fine powder of samples was mixed with KBr and then compressed to form a transparent pellet that was analysed using FT-IR instrument. The spectra obtained were recorded at a wavelength between 400 and 4000 cm^{-1} on the transmittance axis scale.

2.7.2. Scanning Electron Microscope (SEM) Analysis

Microscopic structure and surface morphology of hydrochar, AH, AHSU and SAH were carried out using Scanning Electron Microscope TESCAN VEGA (SEM) operating at an accelerating voltage of 20 Kv. Drying of the samples prepared was done to a constant mass using an oven. The dried samples were ground using a mortar and pestle to obtain fine powder. The samples were then coated with gold and mounted on carbon tape and analyzed using SEM [10].

2.7.3. X-Ray Diffraction (XRD) Analysis

The XRD analysis was performed to determine the phase composition of the hydrochar, AH, AHSU and SAH using a Philips X'Pert instrument at 40 mA with Cuka radiation at 0.1541 nm. A monochromatic beam with a step size of 0.0170 (2θ), a time step of 175.26 s and a scan range of 2θ from 0 - 100° was applied. The prepared samples were dried and ground using a mortar and pestle to obtain fine powder. The dry powdered samples were then mounted on slides and placed in an XRD instrument for analysis [11].

3. Results and Discussions

3.1. FT-IR Analysis

3.1.1. Functional Groups Analysis for Hydrochar

FT-IR technique was used to determine the functional groups of the synthesised hydrochar. **Figure 2** show the IR spectra for the hydrochar.

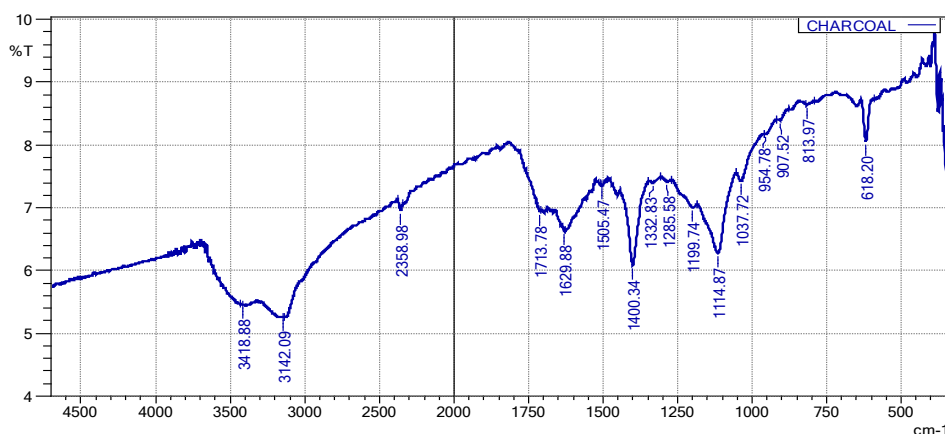


Figure 2. FT-IR spectrum for hydrochar.

The spectrum showed a broad spectral band at 3418.88 cm^{-1} and 3142.09 cm^{-1} ascribed to phenolic and alcoholic -OH groups [12]. The spectral peak at 1713.78 cm^{-1} corresponded to the C=O stretching vibration for an aldehyde group [13]. The intense peaks at 1629.88 cm^{-1} and 618.20 cm^{-1} corresponded to skeletal vibration and bending for the C=C aromatic ring [14] [15]. The sharp intense band at 1400.34 cm^{-1} and also at 954.78 cm^{-1} were associated to -OH groups in and out of plane bending for alcoholic and phenolic groups [16], while the spectral band at 1285.58 cm^{-1} was attributed to C-O asymmetric stretching vibration for ether [17]. The sharp spectral peaks at 1114.87 cm^{-1} and 1037.72 cm^{-1} were ascribed to C-O of the ether, alcoholic and phenolic groups. The spectral band at 813.97 cm^{-1} corresponded to -CH deformation vibration stretch [18].

3.1.2. FT-IR Analysis of the Activated Hydrochar (AH)

The FT-IR technique was used to determine the functional groups of the activated hydrochar. **Figure 3** show the functional groups for the activated hydrochar.

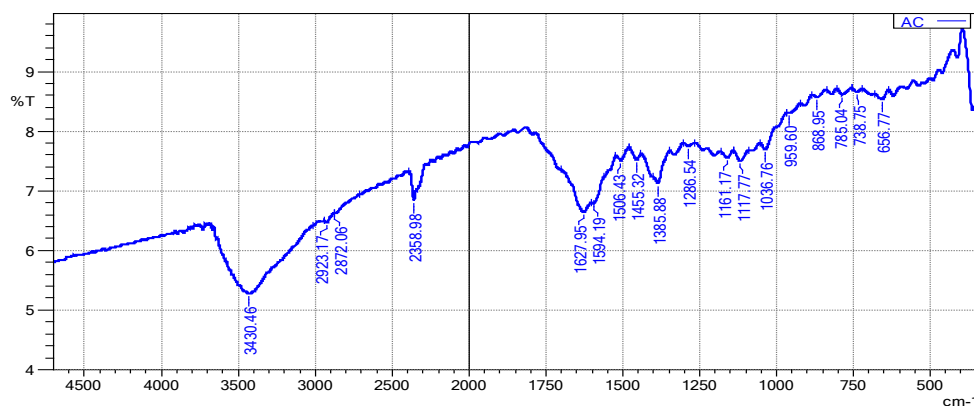


Figure 3. FT-IR spectrum for AH.

A broad intense band of -OH for carboxylic group involved in intermolecular and intramolecular hydrogen bonding shifted from 3418.88 cm⁻¹ to 3430.46 cm⁻¹ [19]. A new peak appeared at 1594.19 cm⁻¹ for carboxylic acid C=O group [20]. This peak showed that oxidation reaction took place by introducing carboxylic functional groups on the surface of the hydrochar.

3.1.3. FT-IR Analysis for AHSU Polymer Units

The functional groups present in the polymer units AHSU was obtained using FT-IR as shown in **Figure 4**.

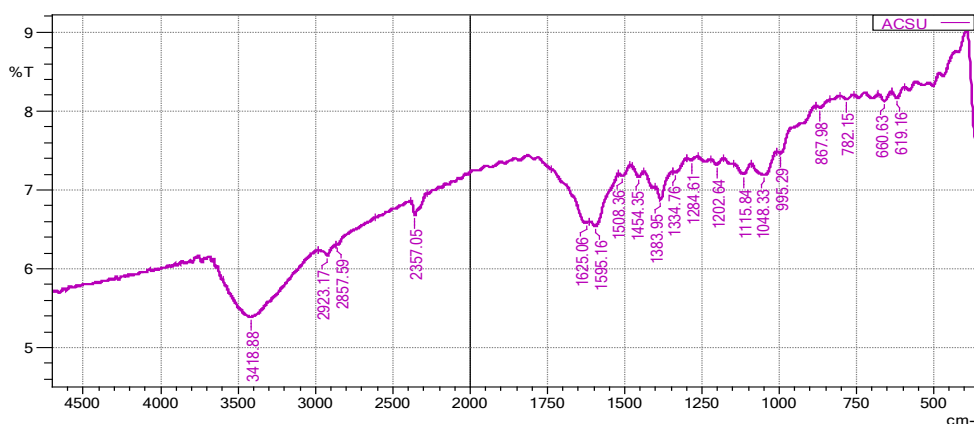


Figure 4. FT-IR spectrum for AHSU.

The spectrum shown by **Figure 4** showed a broad spectral peak at 1625.05 cm⁻¹ ascribed to C=O stretching vibration of the ester and carboxylic acid [21]. The C=O group implied successful polymerization through crosslinking between hydroxyl groups in sucrose (SU) and carboxylic groups in activated hydrochar (AH) forming activated hydrochar sucrose (AHSU) polymer chain units.

3.1.4. FT-IR Characterization of SAH

The FT-IR analysis was carried out to determine functional groups of SAH as shown in the spectrum in **Figure 5**.

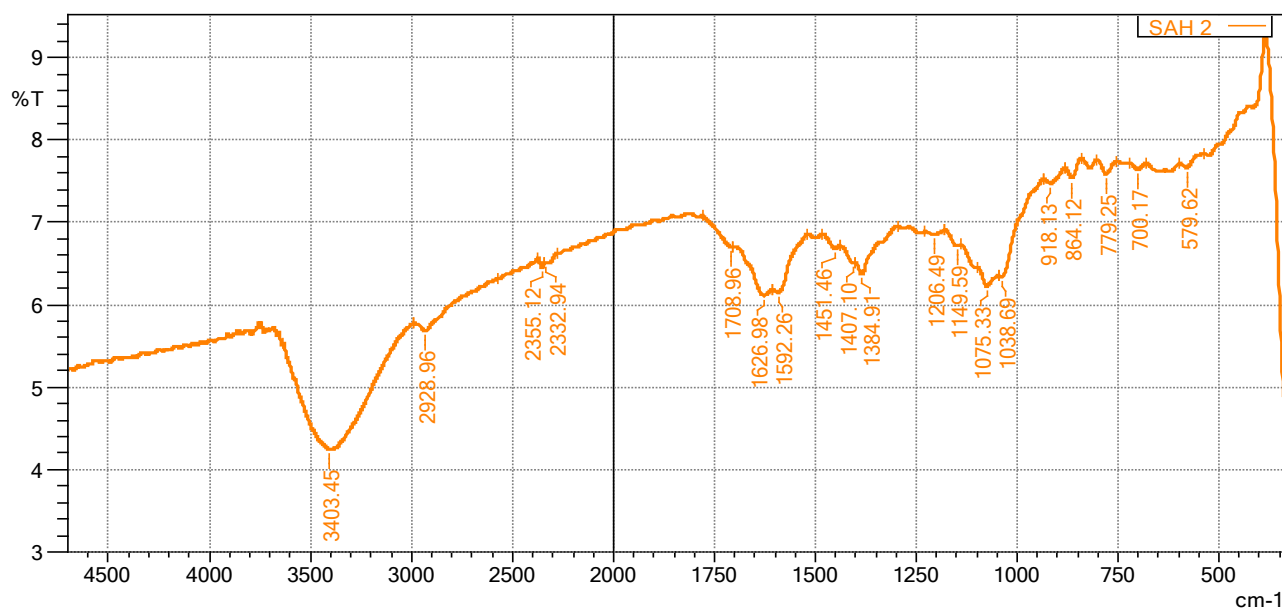


Figure 5. FT-IR spectrum for SAH.

SAH as synthesized by crosslinking AHSU polymer units with maleic acid (MA). FT-IR of SAH showed emergence of a new peak at 1708.96 cm⁻¹ attributed to C=O carbonyl group for the ester [22]. This new peak is an indication that polymer units of AHSU were successfully crosslinked with maleic acid through ester linkage.

3.2. SEM Characterization

The SEM analysis was carried out to determine the surface morphology of the synthesised hydrochar, AH, AHSU and superabsorbent hydrogel SAH. The micrographs in **Figure 6** below show the surface morphology of hydrochar, AH, AHSU and SAH respectively.

The hydrochar micrograph showed smooth layered structures with cracks and a small number of pores (white particles), indicating that the dehydration process created a large surface that was the target for the introduction of oxygen groups during the oxidation process. The AH micrograph showed that upon activation of the hydrochar, the external surface of the AH developed a quasi-cleavage fractured surface with large cavities, a wider pore network, and crater-like surfaces, indicating a higher surface area [23]. This was a result of the introduction of carboxylic groups on carbon chains of hydrochar. Carboxylic groups were required to create ester linkage between the AH monomer and the SU monomer during polymerization. Upon reaction of AH with SU to form AHSU, a micrograph with a rigid cleavage fractured-like surface with unevenly distributed macropores was obtained. However, upon crosslinking of AHSU with MA, dense, evenly distributed micropores and macropores on the surface of SAH were observed. This is a clear indication of successful surface modifications during crosslinking. Rahman *et al.* [24] obtained similar results.

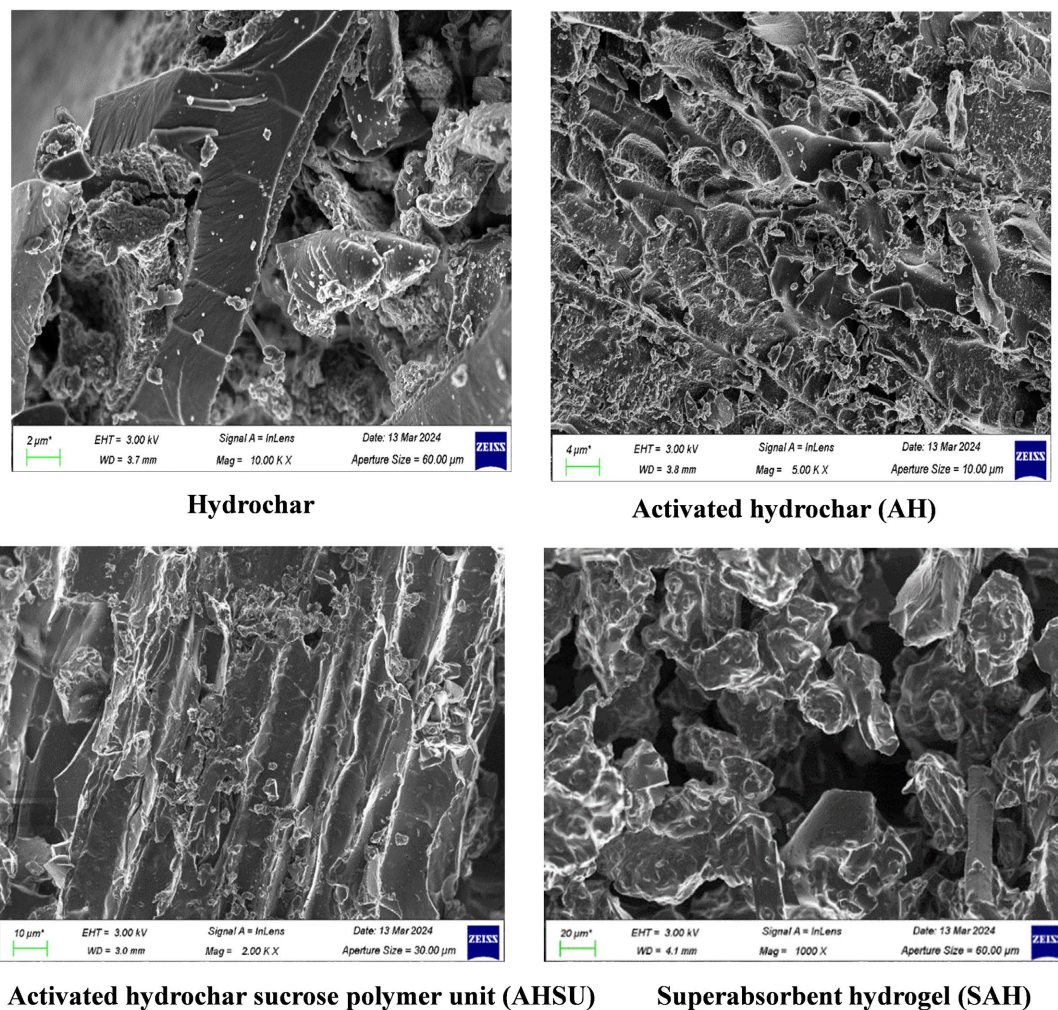


Figure 6. SEM analysis for hydrochar, AH, AHSU and SAH.

3.3. X-Ray Diffraction Analysis

The XRD analysis was carried out to determine the crystalline phase of the synthesized hydrochar, AH, AHSU and SAH as shown on **Figure 7**.

The diffractograms at 2θ angle range of the hydrochar and AH showed that they had single diffused broad hump peaks centred at 25° indicating that they were amorphous [25]. This was due to lignin and hemicellulose presence since they are both amorphous while the cellulose chains that are crystalline were partially destroyed during the dehydration process [26]. The diffractograms for AHSU polymer units and superabsorbent hydrogels SAH showed that they were more crystalline as compared to the amorphous broad hump diffractograms of hydrochar and AH. This was attributed to the carboxylate ions COO^- of AHSU formed by the COOH functional groups of AH and OH groups of SU during polymerization, and the ones formed between the AHSU polymer units and MA during crosslinking [27]. It was also attributed to the increased number of $-\text{OH}$ hydroxyl groups during polymerization of AH and SU and after crosslinking of the AHSU polymer units with MA [28].

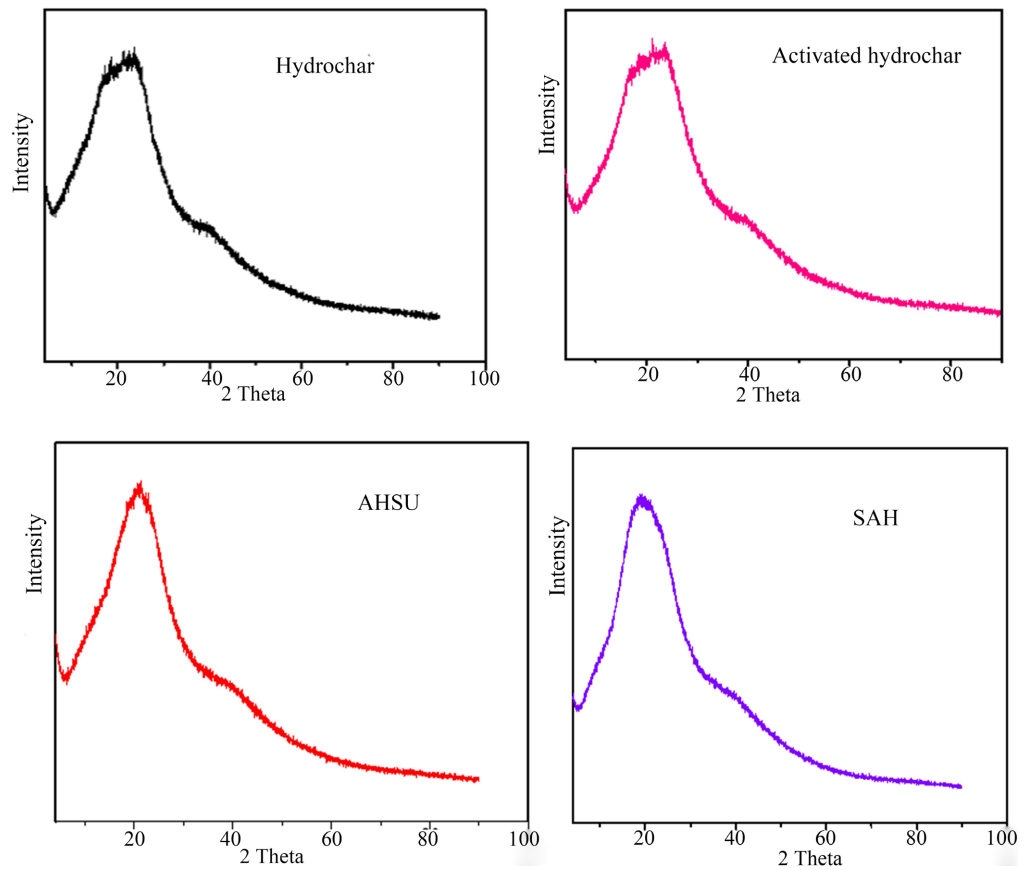


Figure 7. XRD Diffractogram of hydrochar, AH, AHSU and SAH.

3.4. Effect of the Amount of MA Crosslinker on the Swelling Percentage of Superabsorbent Hydrogel (SAH)

The effect of the amount of maleic acid on the swelling percentage of SAH was determined by using the following doses: 1, 2, 3, 4, and 5 g. **Figure 8** was obtained when 2 g of each superabsorbent hydrogel sample synthesized was immersed in distilled water for 24 hours. The mass change was used to determine mean swelling percentages using equation 1.

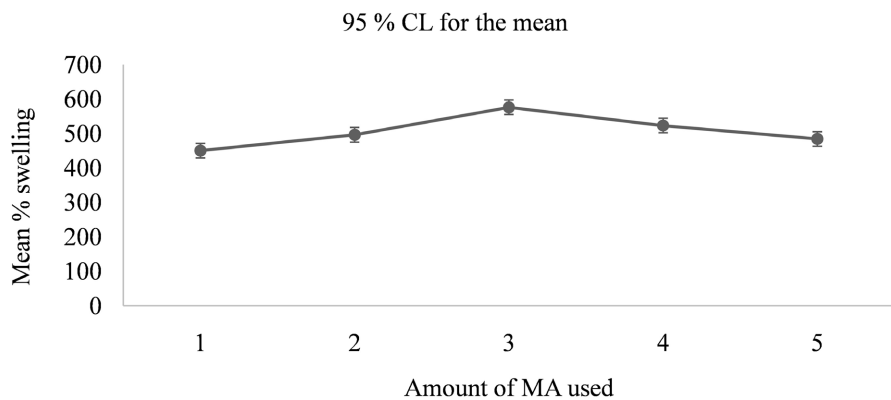


Figure 8. The effect of MA doses on the swelling percentage of 2 g of SAH (10 g AH, 5 g SU and 0.8 g NaOH).

Figure 8 showed that the swelling percentage significantly increased ($p < 0.05$) from 450% to 576% when the concentration of the MA was increased from 1.0 g to 3.0 g, followed by a significant decrease ($p < 0.05$) to 484% as doses increased above 3.0 g. The increase was attributed to the increase of crosslinking joints created between the carboxylic hydrophilic functional groups, creating a polymer skeleton with more sites for water intake [29]. The decrease recorded after the optimal dose of 3 g could be attributed to the interlocking of the hydrogel polymeric chains caused by overcrowding of the crosslinking density that prohibits the expansion of the superabsorbent hydrogels' skeleton during water absorption [30]. Therefore, the optimum dose of MA for the synthesis of superabsorbent hydrogel was found to be 3.0 g.

3.5. Effect of Sucrose Dosage on the Swelling Percentage of Superabsorbent Hydrogel (SAH)

The effect of the amount of SU on the swelling percentage of the synthesized SAH hydrogel was determined by varying the amount of the sucrose in the range of 2, 4, 6, 8, and 10 g. **Figure 9** shows the graph obtained when 2 g of each hydrogel sample was immersed in distilled water for 24 hours. Equation 1 was used to determine swelling percentages of the hydrogels.

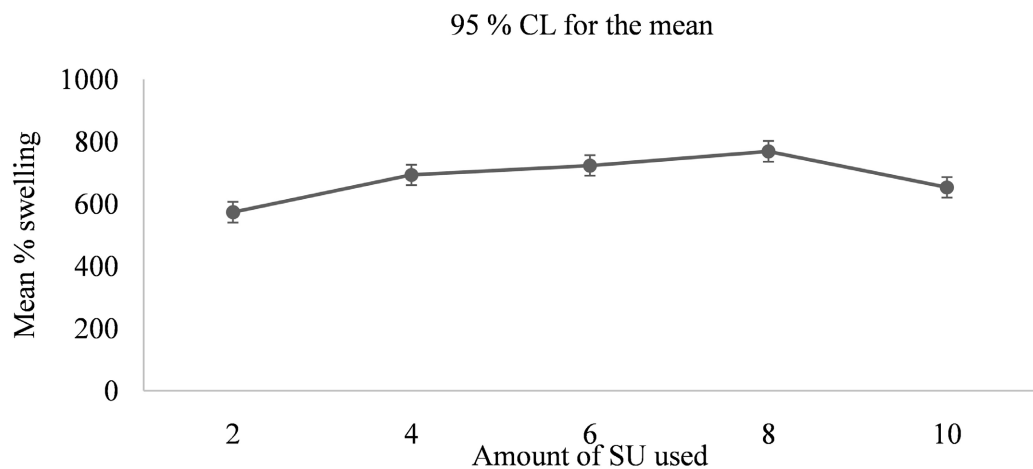


Figure 9. The effect of SU dosage on the swelling percentage of 2 g (SAH) superabsorbent hydrogel (10 g AH, 3 g MA and 0.8 g NaOH).

Figure 9 illustrates that increasing the SU dosage from 2.0 g to 8.0 g resulted in a substantial rise ($p < 0.05$) in swelling percentage from 573% to 769%, followed by a significant decrease ($p < 0.05$) as the dosage increased above 8.0 g. The increase could be attributed to the fact that an increase in the number of hydroxyl groups increases grafting between the monomers, hence elevating the water absorption sites [31]. The decrease in the swelling percentage above the optimum dose is associated with the disproportion between the monomers as the SU became more than the AH monomer [32]. The study obtained an optimal ratio of 10 g AH: 8 g SU: 3 g MA for the preparation of the superabsorbent hydrogel.

3.6. Effect of Contact Time on the Percentage Swelling of the Superabsorbent Hydrogel (SAH)

The effect of the contact time of the superabsorbent hydrogel SAH prepared at optimum conditions was determined by immersing 2.0 g of each hydrogel sample in 600 mL of water and determining swelling capacity at intervals of 0.5, 1, 2, 4, 6, 8, 12 and 24 hours. **Figure 10** below shows the graph of the mean swelling percentage capacity as a function of time (hours) for the superabsorbent hydrogel samples.

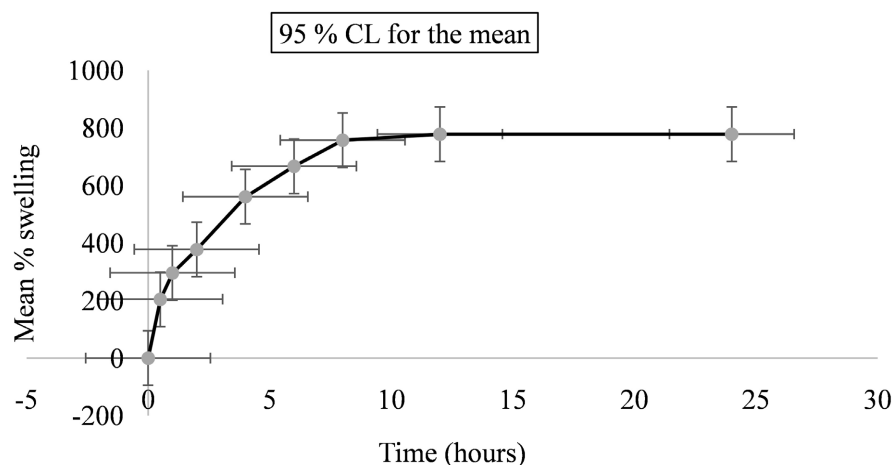


Figure 10. The effect of the contact time of 2 g superabsorbent hydrogel (SAH).

Figure 10 showed a significant increase ($p < 0.05$) in the percentage swelling capacity of SAH from 0 to 8 hours, attaining a maximum swelling capacity of 778%. From 8 to 24 hours, there was no significant increase ($p > 0.05$) in the swelling capacity since equilibrium had been attained. The increase in swelling capacity was attributed to distilled water penetrating the hydrogel's network through diffusion and capillary action, which occurred as the hydrogel transitioned into a glassy state due to the presence of hydrophilic functional groups like hydroxyl and carboxyl groups. The decreased rate of absorption after 12 hours was attributed to the reduction of electrostatic repulsion due to decreased hydrophilic groups through water absorption caused by saturation of the hydrogel's network structure with distilled water [33].

4. Conclusion

The study reports that the superabsorbent hydrogel (SAH) achieved a maximum swelling capacity of 778% using an optimal synthesis ratio of 10:8:3 for AH:SU:MA. FT-IR analysis confirmed successful crosslinking via a spectral band at 1708.96 cm^{-1} , indicative of the C=O carbonyl group. Scanning Electron Microscopy (SEM) illustrated a dense, uniformly porous surface for SAH compared to fewer pores in AHSU polymer units. X-ray Diffraction (XRD) analysis revealed amorphous phases in hydrochar and AH, while both AHSU and SAH exhibited increased crystallinity.

The high-water absorption capacity of SAH suggests its potential application in agriculture, particularly in arid and semi-arid regions.

Acknowledgements

The authors express gratitude to Kenyatta University's chemistry department, department of physical science Machakos university and Kibabii university's science technology and engineering department for the assistance offered during the research period.

Conflicts of Interest

The authors declare that they have no known competing financial interests or personal relationships that could appear to have influenced the work described in this paper.

References

- [1] Karoyo, A.H. and Wilson, L.D. (2021) A Review on the Design and Hydration Properties of Natural Polymer-Based Hydrogels. *Materials*, **14**, Article 1095. <https://doi.org/10.3390/ma14051095>
- [2] Kasimu, T.M., Mbuvi, H.M. and Maingi, F.M. (2024) Green Superabsorbent Hydrogel Derived from Activated Charcoal and Glycerol with Maleic Acid as a Cross-linker. *Journal of Experimental Sciences*, **15**, 1-7. <https://doi.org/10.25081/jes.2024.v15.8767>
- [3] Tan, H. and Marra, K.G. (2010) Injectable, Biodegradable Hydrogels for Tissue Engineering Applications. *Materials*, **3**, 1746-1767. <https://doi.org/10.3390/ma3031746>
- [4] Behera, S. and Mahanwar, P.A. (2019) Superabsorbent Polymers in Agriculture and Other Applications: A Review. *Polymer-Plastics Technology and Materials*, **59**, 341-356. <https://doi.org/10.1080/25740881.2019.1647239>
- [5] Anah, L. and Astrini, N. (2015) Hydrogel Super Absorbent Polymer (SAP) Crosslinking Agent Water-Soluble Carbodiimide (WSC). *Journal Cellulose*, **5**, 1-6. <https://doi.org/10.25269/jsel.v5i01.73>
- [6] Isahak, W.N.R.W., Hisham, M.W.M. and Yarmo, M.A. (2012) Highly Porous Carbon Materials from Biomass by Chemical and Carbonization Method: A Comparison Study. *Journal of Chemistry*, **2013**, Article ID: 620346. <https://doi.org/10.1155/2013/620346>
- [7] Yahya, M.A., Mansor, M.H., Zolkarnaini, W.A.A.W., Rusli, N.S., Aminuddin, A., Mohamad, K., *et al.* (2018) A Brief Review on Activated Carbon Derived from Agriculture By-Product. *AIP Conference Proceedings*, **1972**, Article 030023. <https://doi.org/10.1063/1.5041244>
- [8] Khodami, S., Kaniewska, K., Karbarz, M. and Stojek, Z. (2023) Antioxidant Ability and Increased Mechanical Stability of Hydrogel Nanocomposites Based on N-Iso-propylacrylamide Crosslinked with Laponite and Modified with Polydopamine. *European Polymer Journal*, **187**, Article 111876. <https://doi.org/10.1016/j.eurpolymj.2023.111876>
- [9] Kulkarni, R.V., Mutalik, S., Mangond, B.S. and Nayak, U.Y. (2012) Novel Interpenetrated Polymer Network Microbeads of Natural Polysaccharides for Modified Release of Water Soluble Drug: *In-Vitro* and *In-Vivo* Evaluation. *Journal of Pharmacy and Pharmacology*, **64**, 530-540. <https://doi.org/10.1111/j.2042-7158.2011.01433.x>

- [10] Damiri, F., Bachra, Y. and Berrada, M. (2022) Synthesis and Characterization of 4-Formylphenylboronic Acid Cross-Linked Chitosan Hydrogel with Dual Action: Glucose-Sensitivity and Controlled Insulin Release. *Chinese Journal of Analytical Chemistry*, **50**, Article 100092. <https://doi.org/10.1016/j.cjac.2022.100092>
- [11] Khan, S. and Ranjha, N.M. (2014) Effect of Degree of Cross-Linking on Swelling and on Drug Release of Low Viscous Chitosan/Poly(Vinyl Alcohol) Hydrogels. *Polymer Bulletin*, **71**, 2133-2158. <https://doi.org/10.1007/s00289-014-1178-2>
- [12] Prasannamedha, G., Kumar, P.S., Mehala, R., Sharumitha, T.J. and Surendhar, D. (2021) Enhanced Adsorptive Removal of Sulfamethoxazole from Water Using Biochar Derived from Hydrothermal Carbonization of Sugarcane Bagasse. *Journal of Hazardous Materials*, **407**, Article 124825. <https://doi.org/10.1016/j.jhazmat.2020.124825>
- [13] Cheng, X.Y., Li, X.J., Xu, K., Huang, Q.T., Sun, H.N. and Wu, Y.Q. (2017) Effect of Thermal Treatment on Functional Groups and Degree of Cellulose Crystallinity of Eucalyptus Wood (*Eucalyptus Grandis* × *Eucalyptus Urophylla*). *Forest Products Journal*, **67**, 135-140. <https://doi.org/10.13073/fpj-d-15-00075>
- [14] Isaac, A., de Paula, J., Viana, C.M., Henriques, A.B., Malachias, A. and Montoro, L.A. (2018) From Nano- to Micrometer Scale: The Role of Microwave-Assisted Acid and Alkali Pretreatments in the Sugarcane Biomass Structure. *Biotechnology for Biofuels*, **11**, Article No. 73. <https://doi.org/10.1186/s13068-018-1071-6>
- [15] Moreno-Tovar, R., Terrés, E. and Rangel-Mendez, J.R. (2014) Oxidation and EDX Elemental Mapping Characterization of an Ordered Mesoporous Carbon: Pb(II) and Cd(II) Removal. *Applied Surface Science*, **303**, 373-380. <https://doi.org/10.1016/j.apsusc.2014.03.008>
- [16] Gurten, I.I., Ozmak, M., Yagmur, E. and Aktas, Z. (2012) Preparation and Characterization of Activated Carbon from Waste Tea Using K₂CO₃. *Biomass and Bioenergy*, **37**, 73-81. <https://doi.org/10.1016/j.biombioe.2011.12.030>
- [17] Thu, M., Koshio, S., Ishikawa, M. and Yokoyama, S. (2010) Effects of Supplementation of Dietary Bamboo Charcoal on Growth Performance and Body Composition of Juvenile Japanese Flounder, *Paralichthys olivaceus*. *Journal of the World Aquaculture Society*, **41**, 255-262. <https://doi.org/10.1111/j.1749-7345.2010.00365.x>
- [18] Feng, J., Li, W. and Xie, K. (2023) Research on Coal Structure Using FT-IR. *Journal of China University of Mining and Technology*, **31**, 362-366.
- [19] Hebeish, A., Aly, A., El-Shafei, A. and Zaghoul, S. (2009) Synthesis and Characterization of Cat Ionized Starches for Application in Flocculation, Finishing and Sizing. *Egyptian Journal of Chemistry*, **52**, 73-89.
- [20] Smith, B.C. (2018) The C = O Bond, Part VI: Esters and the Rule of Three. *Spectroscopy*, **33**, 20-23.
- [21] Ghorpade, V.S., Yadav, A.V. and Dias, R.J. (2016) Citric Acid Crosslinked Cyclodextrin/Hydroxypropylmethylcellulose Hydrogel FILMS for hydrophobic Drug Delivery. *International Journal of Biological Macromolecules*, **93**, 75-86. <https://doi.org/10.1016/j.ijbiomac.2016.08.072>
- [22] Demitri, C., Del Sole, R., Scalera, F., Sannino, A., Vasapollo, G., Maffezzoli, A., et al. (2008) Novel Superabsorbent Cellulose-based Hydrogels Crosslinked with Citric Acid. *Journal of Applied Polymer Science*, **110**, 2453-2460. <https://doi.org/10.1002/app.28660>
- [23] Hanum, F., Bani, O. and Wirani, L.I. (2017) Characterization of Activated Carbon from Rice Husk by HCL Activation and Its Application for Lead (Pb) Removal in Car Battery Wastewater. *IOP Conference Series: Materials Science and Engineering*, **180**,

- Article 012151. <https://doi.org/10.1088/1757-899x/180/1/012151>
- [24] Rahman, M.S., Islam, M.M., Islam, M.S., Zaman, A., Ahmed, T., Biswas, S., *et al.* (2019) Morphological Characterization of Hydrogels. In: Mondal, M., Ed., *Polymers and Polymeric Composites: A Reference Series*, Springer International Publishing, 819-863. https://doi.org/10.1007/978-3-319-77830-3_28
- [25] Pradhan, S. (2011) Production and Characterization of Activated Carbon Produced from A Suitable Industrial Sludge. A Project Report, NIT Rourkela.
- [26] Yang, Z., Xu, S., Ma, X. and Wang, S. (2008) Characterization and Acetylation Behavior of Bamboo Pulp. *Wood Science and Technology*, **42**, 621-632. <https://doi.org/10.1007/s00226-008-0194-5>
- [27] Naohara, R., Narita, K. and Ikeda-Fukazawa, T. (2017) Change in Hydrogen Bonding Structures of a Hydrogel with Dehydration. *Chemical Physics Letters*, **670**, 84-88. <https://doi.org/10.1016/j.cplett.2017.01.006>
- [28] Mudgil, D., Barak, S. and Khatkar, B.S. (2012) X-Ray Diffraction, IR Spectroscopy and Thermal Characterization of Partially Hydrolyzed Guar Gum. *International Journal of Biological Macromolecules*, **50**, 1035-1039. <https://doi.org/10.1016/j.ijbiomac.2012.02.031>
- [29] Wei, P., Chen, W., Song, Q., Wu, Y. and Xu, Y. (2021) Superabsorbent Hydrogels Enhanced by Quaternized Tunicate Cellulose Nanocrystals with Adjustable Strength and Swelling Ratio. *Cellulose*, **28**, 3723-3732. <https://doi.org/10.1007/s10570-021-03776-z>
- [30] Das, D., Prakash, P., Rout, P.K. and Bhaladhare, S. (2020) Synthesis and Characterization of Superabsorbent Cellulose-Based Hydrogel for Agriculture Application. *Starch-Stärke*, **73**, Article 1900284. <https://doi.org/10.1002/star.201900284>
- [31] Costa, P. and Sousa Lobo, J.M. (2001) Modeling and Comparison of Dissolution Profiles. *European Journal of Pharmaceutical Sciences*, **13**, 123-133. [https://doi.org/10.1016/s0928-0987\(01\)00095-1](https://doi.org/10.1016/s0928-0987(01)00095-1)
- [32] Mishra, A. and Malhotra, A.V. (2009) Tamarind Xyloglucan: A Polysaccharide with Versatile Application Potential. *Journal of Materials Chemistry*, **19**, Article 8528. <https://doi.org/10.1039/b911150f>
- [33] Rimdusit, S., Somsaeng, K., Kewsuwan, P., Jubsilp, C. and Tiptipakorn, S. (2012) Comparison of Gamma Radiation Crosslinking and Chemical Crosslinking on Properties of Methylcellulose Hydrogel. *Engineering Journal*, **16**, 15-28. <https://doi.org/10.4186/ej.2012.16.4.15>